doi: 10.82124/CEAS-GNC-2026-005 CEAS-GNC-2026-005

A Genetic Algorithm–Based Neuro-Fuzzy Adaptive Computed-Torque Controller for Lower-Limb Rehabilitation Exoskeletons

Muhammad Adel Yusuf Ph.D. Student, King Fahd University of Petroleum and Minerals (KFUPM), Dhahran, Saudi Arabia. muhammad.adel@ejust.edu.eg

Ali Nasir Assistant Professor, King Fahd University of Petroleum and Minerals (KFUPM); Interdisciplinary Research Center for Intelligent Manufacturing and Robotics, Dhahran, Saudi Arabia. ali.nasir@kfupm.edu.sa

Sami El-Ferik Professor, King Fahd University of Petroleum and Minerals (KFUPM); Interdisciplinary Research Center for Smart Mobility and Logistics, Dhahran, Saudi Arabia. selferik@kfupm.edu.sa

ABSTRACT

Due to the growing aging society and the increasing number of people who suffer from lower limb disorders worldwide, the need for robot-assisted gait training devices has become increasingly urgent. These systems are essential for supporting clinicians in rehabilitation and enhancing functional recovery in both upper and lower extremities. However, the significant variability in users' physical characteristics—such as body mass, limb length, and inertia—introduces dynamic uncertainties that challenge conventional control strategies. To address this, we propose a User-Adaptive Genetic Algorithm-Tuned Neuro-Fuzzy (GA-Tuned Neuro-Fuzzy) controller integrated within a Computed Torque Control (CTC) framework. The proposed approach leverages the learning capability of an Adaptive Neuro-Fuzzy Inference System (ANFIS) and the optimization ability of a Genetic Algorithm (GA) to adaptively tune control parameters based on varying anthropometric profiles. Simulation results demonstrate that the controller achieves accurate trajectory tracking, low steady-state error, and robust performance across a wide range of user conditions and reference inputs. These findings validate the effectiveness of the proposed controller for personalized and adaptive rehabilitation in lower limb exoskeleton applications.

Keywords: Rehabilitation, Exoskeleton, Computed Torque Control, ANFIS, Adaptive control, Genetic ALgorithm

Nomenclature

Acronyms

ANNs	=	Artificial Neural Networks
ANFIS	=	Adaptive Neuro-Fuzzy Inference System
CTC	=	Computed Torque Control
GA	=	Genetic Algorithm
ITAE	=	Integral of Time-weighted Absolute Error

LAREX	=	Lower-limb Adjustable Rehabilitation Exoskeleton
LLEx	=	Lower Limb Exoskeleton
SMC	=	Sliding Mode Control

Symbols

$\theta_1, \theta_2, \theta_3$	=	Joint angles of hip, knee, and ankle of the LAREX
m_1, m_2, m_3	=	Masses of links 1, 2, and 3 of the exoskeleton
L_1, L_2, L_3	=	Lengths of links 1, 2, and 3 in the device structure
L_{c1}, L_{c2}, L_{c3}	=	Distances from the center of mass of links 1, 2, and 3 to their respective reference points
I_1, I_2, I_3	=	Moments of inertia of links 1, 2, and 3
$M(q)$	=	Inertia (mass) matrix of the exoskeleton system
$V(q, \dot{q})$	=	Coriolis and centripetal torque vector
$G(q)$	=	Gravitational torque vector
τ_f	=	Dynamic friction torque vector
$F(\dot{q})$	=	Viscous friction torque vector
p_1, p_2	=	Dynamic friction coefficients for Links 1 and 2
v_1, v_2	=	Viscous friction coefficients for Links 1 and 2
$q, \dot{q}, \ddot{q}$	=	Generalized position, velocity, and acceleration vectors
τ	=	Actuated joint torque vector
K_p, K_d	=	Proportional and derivative gain matrices
$e, \dot{e}$	=	Tracking error and its derivative
L	=	Lagrangian function ($L = KE - PE$)
KE	=	Total kinetic energy
PE	=	Total potential energy

1 Introduction

In recent years, the number of individuals suffering from lower limb motor dysfunction—resulting from causes such as accidents, war injuries, sports trauma, spinal cord injuries, and paralysis—has been steadily rising, posing significant challenges to patients' quality of life and increasing the burden on healthcare systems [1]. Gait training, particularly after stroke or spinal cord injury, is a key rehabilitation strategy to aid in functional recovery. Exoskeleton-based rehabilitation robots have emerged as a promising solution, with studies showing their effectiveness in improving gait and balance in stroke patients [2]. These devices enable repetitive, targeted, and high-intensity training of the impaired limbs, contributing to improved motor control and muscular strength [3]. However, the variability in patient profiles presents significant challenges in controlling such systems, often resulting in poor stability and limited adaptability to uncertain user-specific dynamic parameters, which can compromise overall system safety.

Currently, most control methods for lower limb rehabilitation exoskeletons rely heavily on accurate system modeling, which hinders their practical implementation. One widely adopted approach is Computed Torque Control (CTC), a form of inverse dynamics control that has received considerable attention and has been applied extensively in both robotic systems and lower limb rehabilitation robots [4]. CTC is based on simplifying assumptions such as decoupling joint dynamics and linearizing the inherently nonlinear system to facilitate control design and enhance trajectory tracking performance [5]. However, in real-world applications, disturbances and parametric uncertainties arising from the exoskeleton's nonlinear dynamics—combined with varying user-specific parameters such as mass, limb length, and inertia—make it difficult to achieve accurate trajectory tracking while maintaining robustness and low steady-state error [6, 7]. As a result, there is a pressing need for additional control mechanisms to compensate for modeling inaccuracies and ensure smooth, stable motion. Common compensatory strategies include adaptive control [4, 8, 9], fuzzy control [10], and sliding mode control (SMC) [11],

often come at the cost of increased computational complexity [12]. More recently, metaheuristic-assisted adaptive controllers have been explored for multi-DOF lower-limb rehabilitation exoskeletons, with reports of improved tracking performance and robustness against uncertainties and external disturbances [8]. Learning-based models have also been investigated as virtual sensing/estimation tools to capture complex nonlinear relationships in systems where direct modeling or measurement is difficult. For example, neural-network-based virtual sensors have been shown to accurately infer end-effector motion from joint measurements in flexible interconnected manipulators, highlighting the potential of data-driven mappings for improving robustness in uncertain robotic systems [13, 14].

Within the lower-limb exoskeleton domain, the adaptive neuro-fuzzy inference system (ANFIS) has been increasingly adopted as a learning-based mechanism to mitigate uncertainty arising from complex, nonlinear dynamics and imperfect modeling. For instance, Arabiat *et al.* employed ANFIS for system identification and trajectory-tracking control of a powered rehabilitation exoskeleton, motivated by the difficulty of obtaining an accurate analytical model for such nonlinear systems [15]. In a complementary direction, neuro-fuzzy compensation architectures have been proposed in which ANFIS augments a conventional feedback controller to improve robustness. Narayan and Dwivedy designed a neuro-fuzzy compensated PID scheme that explicitly targets parametric uncertainty and unstructured disturbances, and validated robustness by increasing the lower-limb masses (a practical surrogate for inter-subject anthropometric variation) and applying friction-torque disturbances [16]. Beyond direct tracking control, ANFIS has also been integrated into exoskeleton control architectures for gait-phase recognition and switching; Hua *et al.* used ANFIS to analyze plantar pressure signals (and their derivatives) to classify swing versus stance and enable flexible phase-dependent switching during locomotion [17]. Collectively, these studies indicate that ANFIS can be used as a data-driven identifier/controller, as an adaptive compensation module within a conventional control structure, or as a gait-phase decision mechanism, motivating its use in this work to address user-dependent uncertainties induced by variations in anthropometric parameters.

Despite these advances, each class of method retains inherent limitations. Adaptive control often involves a large number of parameters and substantial gain tuning, and it may exhibit elevated transient errors during the initial adaptation phase, which can pose safety concerns in user-assistive rehabilitation scenarios. Robust control strategies, on the other hand, depend on predefined uncertainty bounds; inaccurate or overly conservative bounds can lead to conservative gain selection, reduced tracking accuracy, and undesirable chattering effects [18]. Learning-based approaches, including ANN-based virtual sensing/estimation models, are likewise constrained by the availability and representativeness of training data and may suffer performance degradation when operating conditions deviate from the training distribution (e.g., changes in structural compliance, friction characteristics, or human–robot interaction dynamics). Moreover, their performance is often sensitive to architecture and hyperparameter choices, while limited interpretability and the lack of explicit stability/safety guarantees can complicate their adoption in safety-critical human-in-the-loop rehabilitation systems.

To address the aforementioned challenges, this work proposes a User-Adaptive Genetic Algorithm-Tuned Neuro-Fuzzy (GA-Tuned Neuro-Fuzzy) control strategy that combines the strengths of CTC, Genetic Algorithm (GA) optimization, and ANFIS for lower limb rehabilitation exoskeletons. This hybrid controller is designed to overcome the limitations of conventional approaches by dynamically adjusting control parameters to account for variations in user profiles, system uncertainties, and external disturbances.

The main contributions of this work are as follows:

1) Global anthropometric data on lower limb segment lengths was analyzed to guide the exoskeleton's dimensional design and estimate parameter uncertainties, enabling robust and adaptive control across diverse user profiles.
2) The optimal proportional-derivative (PD) gains for the CTC controller are identified using GA across different user profiles, and the resulting data is collected.

3) An ANFIS model is trained using the collected data to enable adaptive control based on varying user characteristics.

Simulation results demonstrate that the proposed GA-Tuned Neuro-Fuzzy controller achieves superior trajectory tracking accuracy, robustness, and stability compared to conventional PD-CTC, particularly in the presence of model uncertainties.

The rest of the paper is structured as follows: Section 2 describes the dynamics of a 3 DOF lower limb device and the Anthropometric Analysis. In Section 3 the GA-Tuned Neuro-Fuzzy controller approach is presented. Section 4 presents the results and discussion of the proposed controller approach. Finally, the conclusion and recommendations for future research are given in Section 5.

2 System Description

2.1 Description of the exoskeleton structure

Based on the anatomical structure of the human leg, the dynamics of both the human lower limb and the robotic exoskeleton can be modeled using rigid links connected by rotational joints. The device primarily consists of three links—the thigh, shank, and foot—interconnected through three revolute joints corresponding to the hip, knee, and ankle. These joints enable flexion-extension movements in the sagittal plane, driven by actuators positioned at each joint. To represent the system, a simplified schematic of the Lower Limb Exoskeleton (LLEx) is modeled as a 3-DOF planar mechanism, as illustrated in Fig 1. A fixed coordinate frame (X_0, Y_0) is defined at Joint 1 (hip joint). The frame (X_1, Y_1) is attached to the end of Link 1 (thigh) at Joint 2 (knee joint) and rotates with it. Similarly, (X_2, Y_2) is attached to the end of Link 2 (shank) at Joint 3 (ankle joint), rotating with the shank, while (X_3, Y_3) is attached to the end of Link 3 (foot). The rotational axes Z_1, Z_2, and Z_3 are perpendicular to the sagittal plane and correspond to the respective joints. Each local coordinate system—(X_0, Y_0, Z_0), (X_1, Y_1, Z_1), and (X_2, Y_2, Z_2)—forms a right-handed coordinate frame.

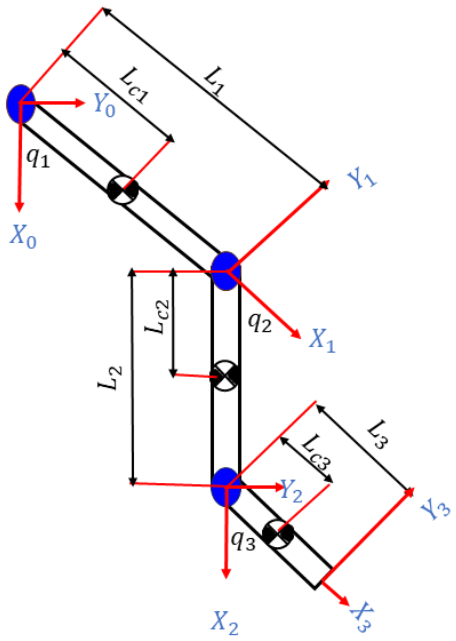

Fig. 1 Schematic diagram of the LLEx.

2.2 Dynamic modeling

To implement the dynamic model of the lower limb exoskeleton, two commonly used approaches are the energy method (Euler–Lagrange) and the momentum method (Newton–Euler). Although the Newton–Euler method is more efficient for real-time control, it involves complex vector cross product operations, making the calculations cumbersome. Therefore, the Euler–Lagrange approach is adopted in this work due to its relatively simpler and more symmetric formulation.

The governing equation for a nonlinear dynamic system using the Euler–Lagrange method is given by:

$$\tau_i = \frac{d}{dt}\left(\frac{\partial L}{\partial \dot{q}_i}\right) - \frac{\partial L}{\partial q_i} \tag{1}$$

where $L = KE - PE$ is the Lagrangian function, KE is the total kinetic energy, PE is the total potential energy, q_i is the generalized coordinate, $\dot{q}_i$ is the generalized velocity and τ_i is the generalized torque.

The general expression for the total kinetic energy is:

$$KE = \frac{1}{2}\left(\sum m_i \, \mathbf{v}_{ci}^T \mathbf{v}_{ci} + \sum \boldsymbol{\omega}_i^T I_{ci} \boldsymbol{\omega}_i\right) \tag{2}$$

The general expression for the total potential energy is:

$$PE = \sum m_i \, \mathbf{g}^T \mathbf{P}_{ci} \tag{3}$$

Based on the Euler–Lagrange formulation, the dynamic model of the 3-DOF lower limb exoskeleton can be expressed as:

$$\tau = M(q)\ddot{q} + V(q, \dot{q}) + G(q) + \tau_f + F(\dot{q}) \tag{4}$$

where $\tau \in \mathbb{R}^{3\times1}$ denotes the actuated input torque vector, $M(q) \in \mathbb{R}^{3\times3}$ is the symmetric positive-definite inertia matrix, and $V(q, \dot{q}) \in \mathbb{R}^{3\times1}$ represents the Coriolis and centripetal torque vector. The term $G(q) \in \mathbb{R}^{3\times1}$ corresponds to the gravitational torque vector, $\tau_f \in \mathbb{R}^{3\times1}$ denotes the dynamic friction torque vector, and $F(\dot{q}) \in \mathbb{R}^{3\times1}$ is the viscous friction torque vector.

The terms in the model are defined as:

$$M(q) = \begin{bmatrix} m_{11} & m_{12} & m_{13} \\ m_{21} & m_{22} & m_{23} \\ m_{31} & m_{32} & m_{33} \end{bmatrix} \tag{5}$$

$$V(q, \dot{q}) = \begin{bmatrix} V_1 \\ V_2 \\ V_3 \end{bmatrix} \tag{6a}$$

$$G(q) = \begin{bmatrix} G_1 \\ G_2 \\ G_3 \end{bmatrix} \tag{6b}$$

$$\tau_f = \begin{bmatrix} p_1 \operatorname{sgn}(\dot{q}_1) \\ p_2 \operatorname{sgn}(\dot{q}_2) \\ 0 \end{bmatrix} \tag{7a}$$

$$F(\dot{q}) = \begin{bmatrix} v_1 \dot{q}_1 \\ v_2 \dot{q}_2 \\ 0 \end{bmatrix} \tag{7b}$$

where v_1 and v_2 are the viscous friction coefficients, and p_1 and p_2 are the dynamic friction coefficients for Link 1 and Link 2, respectively.

2.3 Anthropometric Analysis

In the design and control of lower limb rehabilitation exoskeletons, user-specific physical characteristics—such as height, limb length, and body segment mass—play a critical role in determining the system dynamics. To evaluate the variability and uncertainty of these parameters across the potential user population, a statistical analysis was conducted using the global anthropometric data [19]. Specifically, the average maximum and minimum heights of individuals worldwide were collected and used as a

basis to estimate corresponding segmental parameters for the lower limbs. The analysis revealed that the tallest average male height is 184 cm in the Netherlands, while the shortest average female height is 152 cm in Guatemala. Additionally, the highest average body weight—104.2 kg—was recorded for men in American Samoa (average height: 177 cm), whereas the lowest—50.3 kg—was for women in East Timor (average height: 152 cm). This variation in height among individuals underscores the need for a robust adaptive controller that can be easily adjusted its parameters to accommodate different users, ensuring accurate and safe rehabilitation therapy.

In order to model the physical parameters of the lower limbs, established biomechanical models were employed. Segment lengths (thigh, shank, and foot) were estimated using parametric scaling models, where each segment is represented as a percentage of the individual's total height [20]. These segmental proportions are illustrated in Fig 2 and listed in Table 1. Similarly, body segment masses were computed based on normalized distribution values reported by Winter [21], as summarized in Table 2. By estimating the lengths and masses of key lower limb segments across the global extremes of height and weight, this study defines the range of dynamic parameter variability the exoskeleton must accommodate. Therefore, this uncertainty could be incorporated into the control design, enabling the development of a robust, adaptive controller that ensures consistent, safe, and effective performance across diverse user profiles.

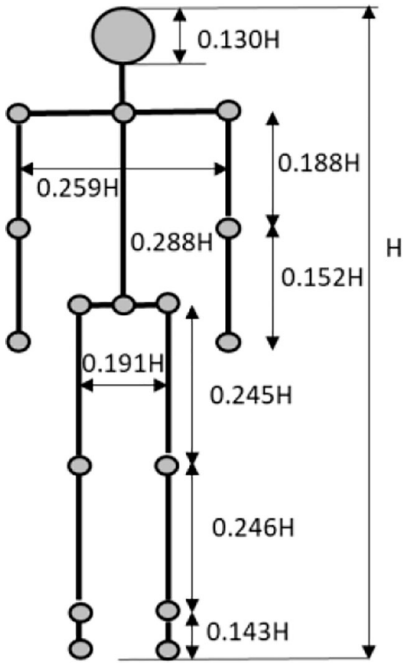

Fig. 2 Percentages of the individual's height [20].

Table 1 Length parameters of human segments as percentages of height

Segment	Length Parameter	Min (m)	Max (m)	Range (cm)
Thigh	$0.245H$	3.724E – 01	4.508E – 01	7.84
Shank	$0.246H$	3.739E – 01	4.526E – 01	7.872
Foot	$0.039H$	5.928E – 02	7.176E – 02	1.248
Waist	$0.191H$	2.903E – 01	3.514E – 01	6.112

Table 2 Mass parameters of human body segments

Segment	Segment Mass / Total Body Mass	Min (kg)	Max (kg)	Range (kg)
Thigh	1.00E – 01	5.03	1.04E + 01	5.37
Shank	4.65E – 02	2.34	4.836	2.496
Foot	1.45E – 02	7.29E – 01	1.51	7.79E – 01

3 Control Architecture

3.1 Computed Torque Control

The CTC is one of the most widely used controllers in robotic systems, leveraging inverse dynamics to calculate the joint torques required for accurate trajectory tracking, particularly under varying and

time-dependent motion trajectories. This controller approach aims to achieve feedback linearization of the non-linear system. This effectively compensates for the gravitational and Coriolis-centripetal force components, as well as eliminates the position-dependent inertia effects. As a result, the control input focuses mainly on tracking performance. By canceling the non-linear dynamics, the system is transformed into a linear form, allowing a conventional linear controller—such as a PD controller as illustrated in Fig.3-to be effectively applied for trajectory tracking.

The PD control law based on the computed torque approach can be expressed as:

$$\tau = M(q)\left(\ddot{q}_d + K_d\dot{e} + K_p e\right) + V(q,\dot{q}) + G(q) + \tau_f \tag{8}$$

where the tracking error is defined as $e = q_d - q_a$ and $\dot{e} = \dot{q}_d - \dot{q}_a$.

Although CTC offers the advantage of precise trajectory tracking and effective linearization of nonlinear dynamics, it is highly dependent on the accuracy of the dynamic model. In practical scenarios, especially in the rehabilitation process, uncertainties in user-specific parameters—such as segment mass and limb length—can significantly degrade performance and potentially lead to instability, compromising user safety. To address this limitation, GA-Tuned Neuro-Fuzzy controller is employed to obtain the optimal PD control gains based on a wide range of user profiles derived from anthropomorphism. These optimized gains allow the development of a robust and user-adaptive control strategy that ensures accurate and stable trajectory tracking performance.

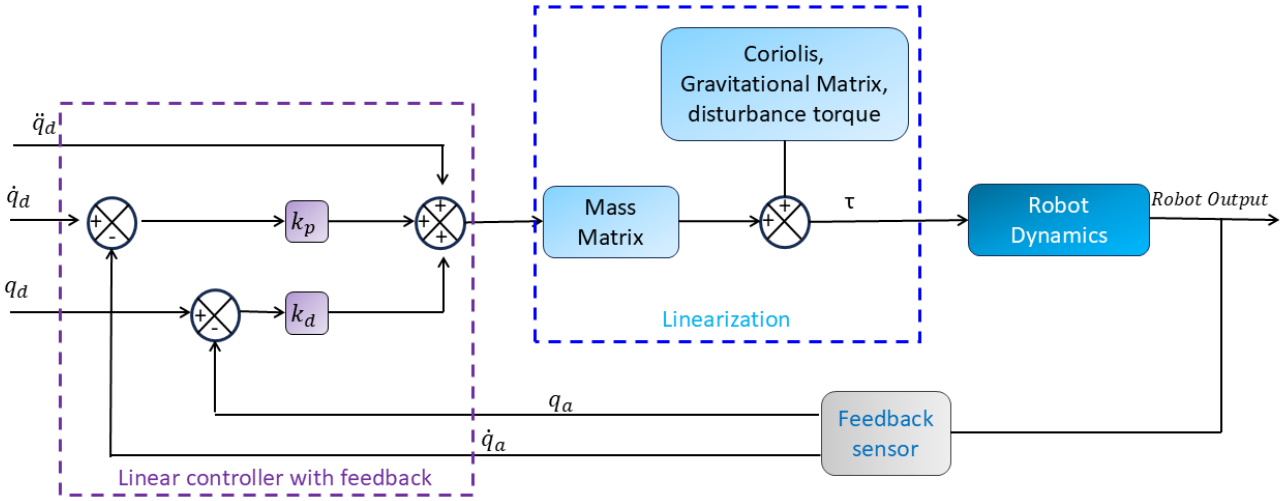

Fig. 3 Schematic Diagram of CTC

3.2 GA-Tuned Neuro-Fuzzy controller

Neuro-fuzzy systems combine the strengths of Artificial Neural Networks (ANNs) and fuzzy logic systems to overcome their individual limitations. ANNs are powerful universal function approximators capable of learning complex nonlinear mappings from input/output data pairs, but their internal structure is often opaque and difficult to interpret. In contrast, fuzzy systems offer transparent and linguistically interpretable rule-based models, allowing designers to understand and control the behavior of the system. However, fuzzy systems face challenges in rule generation, especially in multi-dimensional or uncertain environments. The integration of both approaches, termed as an Adaptive neuro-fuzzy system (ANFIS), leverages the learning capability of neural networks with the interpretability of fuzzy logic. ANFIS consists of fuzzy IF-THEN rules with associated membership functions (MFs). These functions are tuned using neural learning algorithms instead of tuning them manually which allows ANFIS to approximate complex nonlinear functions while adapting to changing inputs and disturbances. It is considered a universal estimator that offers both precision and interpretability [22, 23].

To overcome the limitations of conventional CTC and ANFIS models in the presence of user-dependent uncertainties, a GA-Tuned Neuro-Fuzzy is proposed. This approach enhances the adaptability and robustness of the control system by integrating optimal and adaptive ANFIS model into the CTC loop.

The implementation of the GA-Tuned Neuro-Fuzzy architecture involves several stages:

Initially, GA is employed to optimize the PD gains of the conventional PD-CTC controller across a wide range of user profiles derived from anthropometric data, as discussed in Section 2. This process generates a dataset of optimal control responses that reflect the dynamic behavior of users with varying physical characteristics, such as height, weight, and limb length. In order to evaluate and guide the optimization, the Integral Total Absolute Error (ITAE) is adopted as the fitness function, due to its effectiveness in reducing overshoot and oscillatory behavior compared to other performance indices. The ITAE is defined as:

$$\text{ITAE} = \int_0^\infty t\,|e(t)|\;dt \tag{9}$$

Secondly, At each set of optimized PD gain values corresponding to a specific user profile, time-series data is collected to construct a training dataset for the ANFIS model. Specifically, the tracking error $e = q_d - q_a$ and its derivative $\dot{e} = \dot{q}_d - \dot{q}_a$ are recorded as input features, while the corresponding control signal

$$v = K_d\dot{e} + K_p e$$

is captured as the target output. This dataset effectively encodes the optimal control behavior across diverse user conditions.

Finally, The trained GA-ANFIS model subsequently replaces the fixed-gain PD controller within the CTC loop, as shown in Fig. 4.

Unlike conventional controllers, the GA-ANFIS-based component dynamically adapts its output based on the user's profile and real-time system states. Consequently, the proposed GA-Tuned Neuro-Fuzzy architecture can effectively compensate for system nonlinearities, parameter uncertainties, and inter-user variability—thereby delivering accurate, robust, and personalized rehabilitation assistance without the need for manual controller re-tuning.

To clearly describe the hybrid integration, the proposed controller preserves the inverse-dynamics structure of CTC while replacing the fixed-gain PD action (8) by an ANFIS-based adaptive action:

$$v_{\text{ANFIS}}(t) = f_\Theta(\phi(t))\,, \qquad \phi(t) = \begin{bmatrix} e(t) \\ \dot{e}(t) \end{bmatrix}, \tag{10}$$

where $f_\Theta(\cdot)$ denotes the ANFIS mapping parameterized by Θ.

Accordingly, the proposed GA–ANFIS CTC law is defined as

$$\tau = M(q)\,(\ddot{q}_d + v_{\text{ANFIS}}) + V(q,\dot{q}) + G(q) + \tau_f + F(\dot{q}). \tag{11}$$

This structure maintains the beneficial model-based cancellation of CTC while using ANFIS to generate an adaptive feedback term that reflects optimal tuning across diverse user profiles.

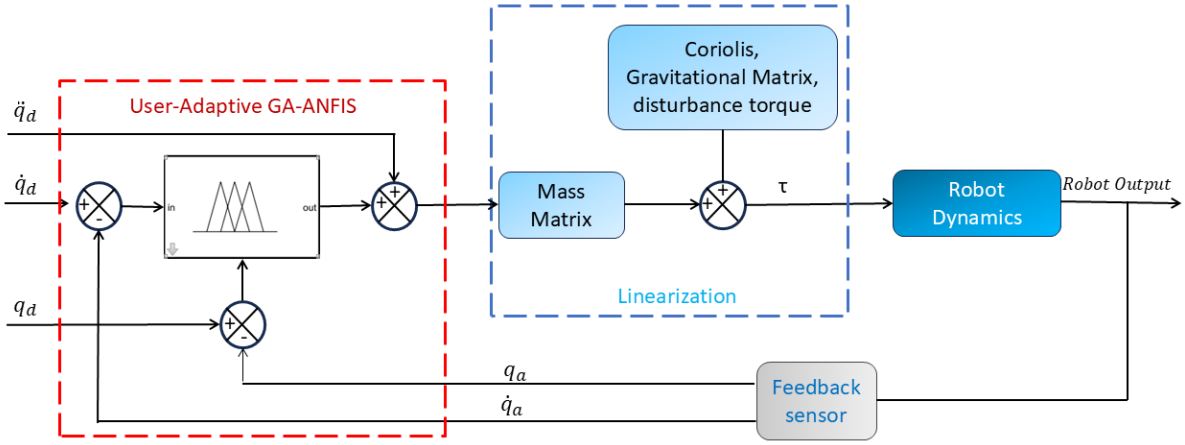

Fig. 4 Schematic Diagram of CTC

4 Results and Discussion

In order to evaluate the effectiveness of the proposed GA-Tuned Neuro-Fuzzy, a series of simulations were conducted using MATLAB R2024b. Initially, the average anthropometric parameters of the human lower limb segments, as presented in Table 3, were used to evaluate the controller's performance under a step input with an amplitude of π radians. It is worth noting that the distance from the joint to the center of mass of each limb segment is assumed to be half of the segment's total length in this experiment. The resulting performance metrics, shown in Fig. 5 and summarized in Table 4, demonstrate that the proposed controller achieves a fast rise time, minimal steady-state error, and low overshoot, highlighting its ability to provide accurate and stable control.

Table 3 Average anthropometric parameters of lower limb segments

Parameter	Thigh	Shank	Foot
Mass m [kg]	7.5	3.5	1.1
Length L [m]	0.42	0.45	0.26
Moment of inertia I [kg·m^2]	0.08	0.09	0.07

Table 4 Step response parameters for the three active joints of the human lower limb

Joint	Rise Time (s)	Settling Time (s)	Overshoot (%)	Steady-State Error (rad)
Hip	9.61E − 02	1.45E + 00	7.42	6.0E − 04
Knee	9.75E − 02	1.46E + 00	7.29	4.0E − 04
Ankle	9.75E − 02	1.47E + 00	7.76	5.0E − 04

Subsequently, the controller has been evaluated using step inputs with varying amplitudes to assess its adaptability and stability across a range of motion demands. This evaluation simulates different levels of joint displacement, representing various challenging rehabilitation scenarios and movement intensities. The proposed User Adaptive GA-Tuned Neuro-Fuzzy controller consistently maintained accurate tracking performance, as demonstrated in Fig. 6, demonstrating low overshoot, fast rise time and negligible steady-state error across all test cases. These results confirm the controller's robustness and its ability to generalize effectively across different reference magnitudes, making it well-suited for patient-specific rehabilitation where joint angle requirements may vary significantly.

Finally, the adaptability of the proposed controller to the varying nature of human profiles was evaluated using three distinct sets of anthropometric parameters, representing the minimum, average,

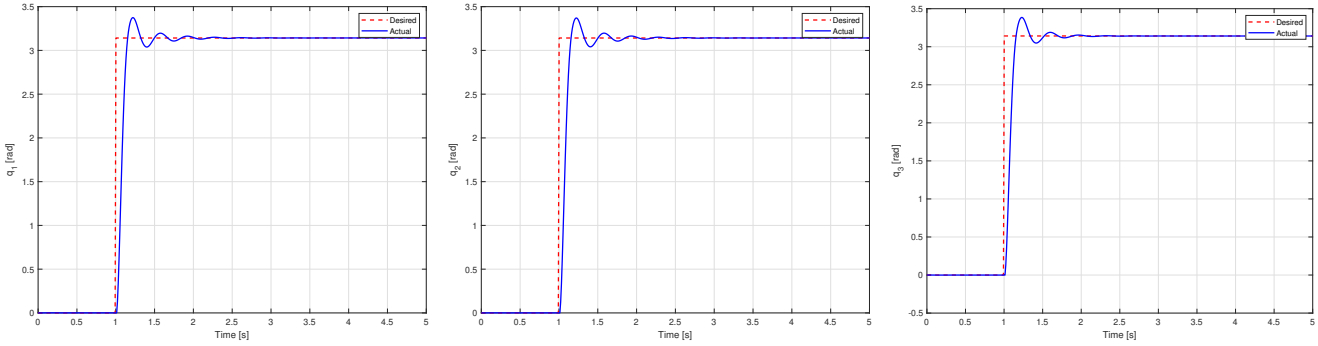

(a) Hip **(b) Knee** **(c) Ankle**

Fig. 5 Step responses for: (a) Hip, (b) Knee, and (c) Ankle joints.

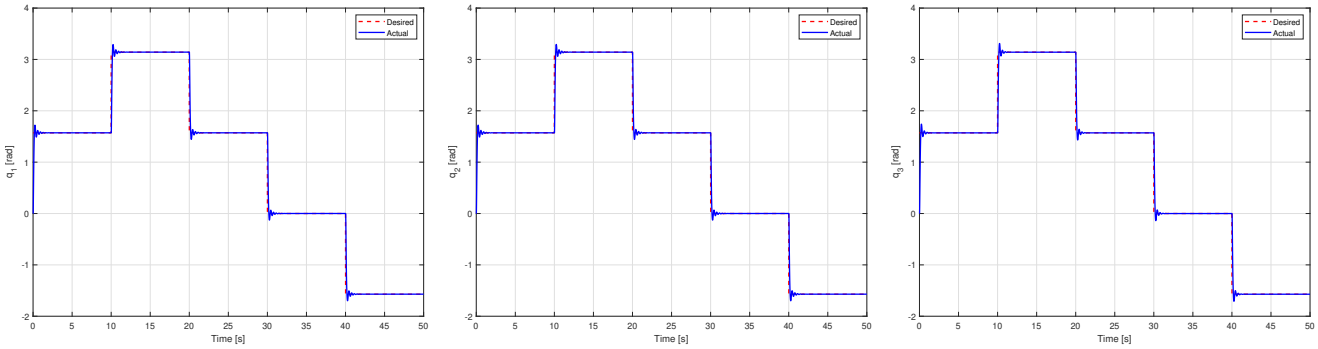

(a) Hip **(b) Knee** **(c) Ankle**

Fig. 6 Tracking Performance Under Step Inputs with Different Amplitudes for: (a) Hip, (b) Knee, and (c) Ankle joints.

and maximum expected human body configurations, as detailed in Table 5. These profiles were selected to capture real-world variability in lower limb segment lengths and masses among different users. As illustrated in Fig 7, the GA-Tuned Neuro-Fuzzy controller demonstrated stable and consistent performance across all parameter sets. It maintained accurate trajectory tracking, exhibited minimal steady-state error, and generated smooth control signals, regardless of the anthropometric variation. These results highlight the robustness and adaptability of the proposed control approach and affirm its effectiveness for personalized rehabilitation applications, where patient-specific dynamics can vary significantly.

Table 5 Anthropometric parameter sets for simulation

Parameter	Min Profile	Avg Profile	Max Profile
m_1 [kg]	5.03	7.50	1.04E + 01
m_2 [kg]	2.34	3.50	4.84
m_3 [kg]	7.29E – 01	1.10	1.50
l_1 [m]	3.72E – 01	4.20E – 01	4.51E – 01
l_2 [m]	3.74E – 01	4.50E – 01	4.53E – 01
l_3 [m]	5.90E – 02	6.50E – 02	7.00E – 02

5 Conclusion

In this paper, a GA-Tuned Neuro-Fuzzy Controller was proposed and integrated into the CTC framework to enhance the adaptability and robustness of lower limb rehabilitation exoskeletons. The

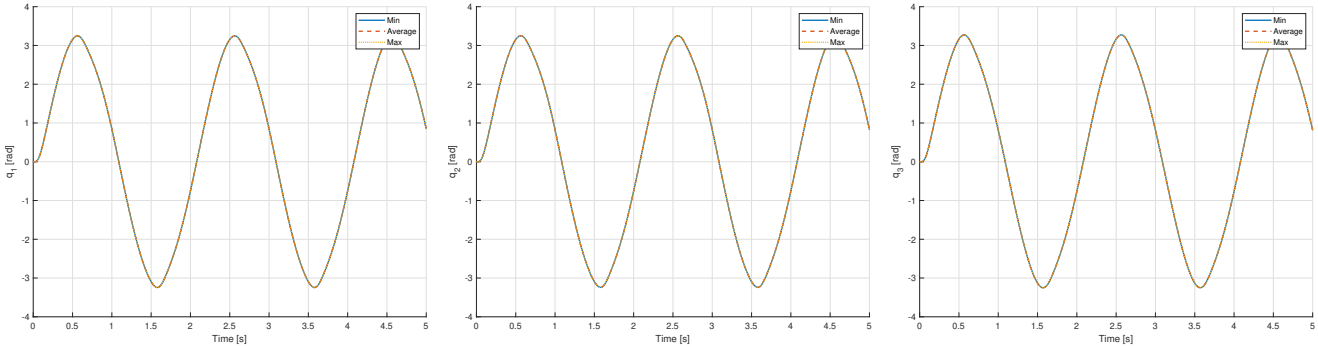

(a) Hip **(b) Knee** **(c) Ankle**

Fig. 7 Performance of GA-Tuned Neuro-Fuzzy Controller for Diverse Anthropometric Configurations for: (a) Hip, (b) Knee, and (c) Ankle joints.

approach leverages the learning capability of neural networks, the interpretability of fuzzy logic, and the optimization power of genetic algorithms to provide a user-adaptive control strategy capable of handling uncertainties in human dynamics. Simulation results demonstrated that the proposed GA-Tuned Neuro-Fuzzy controller achieves fast rise times, minimal steady-state errors, and low overshoot across a wide range of operating conditions. The controller consistently maintained accurate trajectory tracking under varying reference inputs and anthropometric profiles, highlighting its potential for personalized rehabilitation applications. By incorporating user-specific dynamics into the control strategy, the system can adapt to different patient profiles without requiring manual retuning, thus improving safety, comfort, and effectiveness. Future work will focus on real-time implementation and experimental validation using a physical exoskeleton platform, as well as extending the approach to include human-in-the-loop adaptation and intent recognition for enhanced rehabilitation outcomes.

References

[1] Xunju Ma, Xingguo Long, Zefeng Yan, Can Wang, Ziming Guo, and Xinyu Wu. Real-time active control of a lower limb exoskeleton based on semg. In *2019 IEEE/ASME international conference on advanced intelligent mechatronics (AIM)*, pages 589–594. IEEE, 2019.

[2] Federica Baronchelli, Chiara Zucchella, Mariano Serrao, Domenico Intiso, and Michelangelo Bartolo. The effect of robotic assisted gait training with lokomat® on balance control after stroke: systematic review and meta-analysis. *Frontiers in neurology*, 12:661815, 2021.

[3] Lutong Li, Qiang Fu, Sarah Tyson, Nick Preston, and Andrew Weightman. A scoping review of design requirements for a home-based upper limb rehabilitation robot for stroke. *Topics in stroke rehabilitation*, 29(6):449–463, 2022.

[4] Junpeng Wu, Jinwu Gao, Rong Song, Rihui Li, Yaning Li, and Lelun Jiang. The design and control of a 3dof lower limb rehabilitation robot. *Mechatronics*, 33:13–22, 2016.

[5] Jinzhu Peng and Yan Liu. Adaptive robust quadratic stabilization tracking control for robotic system with uncertainties and external disturbances. *Journal of Control Science and Engineering*, 2014(1):715250, 2014.

[6] Mojtaba Sharifi, Javad K Mehr, Vivian K Mushahwar, and Mahdi Tavakoli. Autonomous locomotion trajectory shaping and nonlinear control for lower limb exoskeletons. *Ieee/ASME Transactions on Mechatronics*, 27(2):645–655, 2022.

[7] Zhijun Li, Kuankuan Zhao, Longbin Zhang, Xinyu Wu, Tao Zhang, Qinjian Li, Xiang Li, and Chun-Yi Su. Human-in-the-loop control of a wearable lower limb exoskeleton for stable dynamic walking. *IEEE/ASME transactions on mechatronics*, 26(5):2700–2711, 2020.

[8] Muhammad Adel Yusuf, Sami El-Ferik, Ali Nasir, and Abdul-Wahid A Saif. Adaptive gwo-based controller for a 3-dof lower limb rehabilitation exoskeleton with an innovative length adjustment mechanism. *Applied Soft Computing*, page 114893, 2026.

[9] Yunlang Xu, Chenyang Ding, Xinyi Su, Zhi Li, and Xiaofeng Yang. Predictive-adaptive sliding mode control method for reluctance actuator maglev system. *Nonlinear Dynamics*, 111(5):4343–4356, 2023.

[10] Richa Sharma, Prerna Gaur, Shaurya Bhatt, and Deepak Joshi. Optimal fuzzy logic-based control strategy for lower limb rehabilitation exoskeleton. *Applied Soft Computing*, 105:107226, 2021.

[11] Anjali S Nair and D Ezhilarasi. Performance analysis of super twisting sliding mode controller by adams–matlab co-simulation in lower extremity exoskeleton. *International Journal of Precision Engineering and Manufacturing-Green Technology*, 7(3):743–754, 2020.

[12] Yanxin Lin. A type ii fuzzy pid controller for lower limb rehabilitation exoskeleton robot. In *2024 5th International Conference on Computer, Big Data and Artificial Intelligence (ICCBD+ AI)*, pages 617–621. IEEE, 2024.

[13] Muhammad Adel, Sabah M Ahmed, and Mohamed Fanni. Predicting the motion of the end effector in a flexible interconnected manipulator with neural networks. In *2022 13th Asian Control Conference (ASCC)*, pages 907–913. IEEE, 2022.

[14] Muhammad Adel, Sabah M Ahmed, and Mohamed Fanni. End-effector position estimation and control of a flexible interconnected industrial manipulator using machine learning. *Ieee Access*, 10:30465–30483, 2022.

[15] Ayeh Arabiat, Mohammad Matahen, Omar Abu Zaid, and Moudar Zgoul. Control of an exoskeleton for lower limb rehabilitation using anfis. *International Journal of Online & Biomedical Engineering*, 18(15), 2022.

[16] Jyotindra Narayan and Santosha Kumar Dwivedy. Towards neuro-fuzzy compensated pid control of lower extremity exoskeleton system for passive gait rehabilitation. *IETE Journal of Research*, 69(2):778–795, 2023.

[17] Yuxiang Hua, Jizhuang Fan, Gangfeng Liu, Xuehe Zhang, Mingzhu Lai, Mo Li, Tianjiao Zheng, Guoan Zhang, Jie Zhao, and Yanhe Zhu. A novel weight-bearing lower limb exoskeleton based on motion intention prediction and locomotion state identification. *IEEE Access*, 7:37620–37638, 2019.

[18] Linlin Nie, Miaolei Zhou, Wenjing Cao, and Xiaoliang Huang. Improved nonlinear extended observer based adaptive fuzzy output feedback control for a class of uncertain nonlinear systems with unknown input hysteresis. *IEEE Transactions on Fuzzy Systems*, 31(10):3679–3689, 2023.

[19] WorldData.info. Average height for men and women worldwide, 2025. Accessed: 26-February-2025. `https://www.worlddata.info/average-bodyheight.php`.

[20] Jnana Sai Abhishek Varma Gokaraju, Weon Keun Song, Min-Ho Ka, and Somyot Kaitwanidvilai. Human and bird detection and classification based on doppler radar spectrograms and vision images using convolutional neural networks. *International Journal of Advanced Robotic Systems*, 18(3):17298814211010569, 2021.

[21] David A Winter. *Biomechanics and motor control of human movement*. John wiley & sons, 2009.

[22] J-SR Jang. Anfis: adaptive-network-based fuzzy inference system. *IEEE transactions on systems, man, and cybernetics*, 23(3):665–685, 1993.

[23] Dervis Karaboga and Ebubekir Kaya. Adaptive network based fuzzy inference system (anfis) training approaches: a comprehensive survey. *Artificial intelligence review*, 52(4):2263–2293, 2019.